ELSEVIER

Journal of Nuclear Materials 266–269 (1999) 1134–1138

journal of nuclear materials

Trace tritium and the H-mode density limit

G.F. Matthews [a,*], K.-D. Zastrow [a], P. Andrew [a], B. Balet [a], N.P. Basse [a], J. Ehrenberg [a], S.K. Erents [b], H. Guo [a], N. Jarvis [a], M. Loughlin [a], F. Marcus [a], R. Monk [a], M. O'Mullane [a], L. Lauro-Taroni [a], G. Sadler [a], G. Saibene [a], R. Simonini [a], P.C. Stangeby [c], J. Strachan [d], A. Taroni [a]

[a] *JET Joint Undertaking, Abingdon, Oxfordshire, OX14 3EA, UK*
[b] *UKAEA Fusion, Culham (UKAEA/EURATOM Fusion Association), Abingdon, Oxon., OX14 3DB, UK*
[c] *Institute for Aerospace Studies, University of Toronto, Canada*
[d] *Plasma Physics Laboratory, Princeton University, Princeton, NJ 08543, USA*

Abstract

Trace amounts of tritium gas have been injected in short puffs into JET ELMy H-modes with a wide range of deuterium gas-fuelling rates. Analysis of the subsequent time evolution of the neutron profile and extraction of the particle transport coefficients have allowed us to distinguish between broad classes of mechanism which have been suggested as explanations for the H-mode density limit. The high penetration probability (~20%) and rapid transport ($\sim\tau_E$) of fuel ions are shown to be only weakly influenced by strong gas fuelling – hence mixture control is possible even when the total electron content is clamped.

Keywords: Density limit; H-mode; Cross-field diffusion

1. Introduction

A critical issue for ITER is that the operating density which is required for ignition is above the Greenwald density limit, $\bar{n}_{e,GL}$ [1] $\bar{n}_{e,GL} = 10^{14} I_p/(\pi a^2)$ (SI units), where I_p is the plasma current and a is the minor radius. For ignition, ITER must achieve a density $\geqslant 1.1 \times \bar{n}_{e,GL}$, [2]. In ELMy H-modes in JET, and other tokamaks, the density is weakly dependent on gas fuelling rate and eventually saturates at about 90% of the Greenwald density limit [3] (Fig. 1). Three distinct explanations have been advanced for H-mode density saturation:

1. At high fuelling rates, fuelled particles find it increasingly difficult to penetrate the H-mode transport barrier either as ions or neutrals and so the density saturates.
2. Particle transport degrades in proportion to the rise in ionisation sources. The saturation is then caused by higher losses at higher fuelling rates.
3. Separatrix density saturates with fuelling rate as a result of detachment in the SOL [4]. If there is also a fairly rigid relationship between separatrix and pedestal density then saturation of the separatrix density implies clamping of the core density.

Short puffs of tritium were used as test particles during a deuterium fuelling scan. Tritons are ideal test particles since they are very similar to the principal plasma species, yet their progress through the plasma can be monitored using neutron detectors. We present an analysis of these discharges which allows us to identify which the degree to which each of the three broad classes of mechanism are responsible for density clamping in H-mode.

2. Trace tritium experiment and analysis

Trace amounts of tritium (1–2% of the deuterium content) were introduced in short puffs (~40 ms) into the

* Corresponding author. Tel.: +44 1235 464 523; +44 1235 464 766; e-mail: gfm@jet.uk.

0022-3115/99/$ – see front matter
PII: S0022-3115(98)00858-7

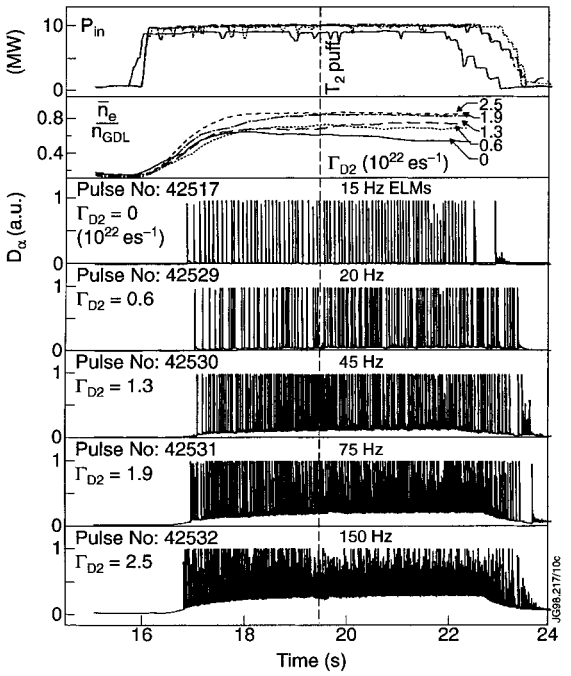

Fig. 1. A series of 2 MA/2 T plasmas with different deuterium fuelling rates (Γ_{D_2} in e/s). The density saturates at ~90% of the Greenwald value.

low field mid-plane edge of the steady-state phase of deuterium plasmas (Fig. 2). The transport properties of the edge and core plasma, and the dynamic tritium recycling, determine the evolution in space and time of the

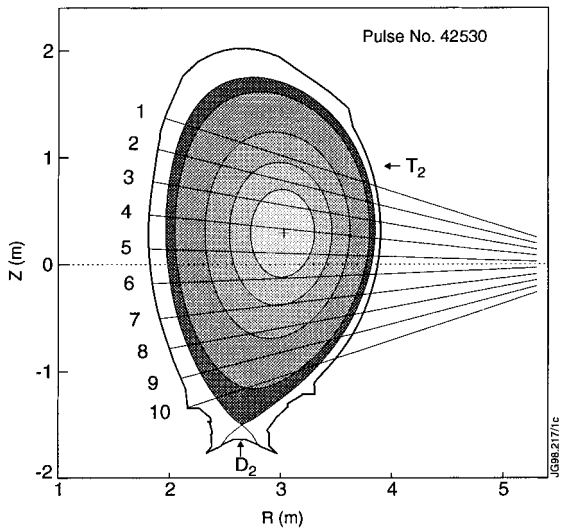

Fig. 2. Viewing geometry of the neutron profile monitor and gas-puff locations for the D_2 and T_2 gas puffing used in the pulses of Fig. 1. The five shaded regions correspond to the independent zones where the transport is modelled.

14 MeV neutron emission following these puffs. The horizontal camera of the JET neutron profile monitor [5] measured the line integral and total neutron emission along 10 independent chords (Fig. 2).

Using the neutron data and its known statistical and channel to channel neutron measurement errors, the triton transport coefficients and their confidence intervals were computed from a least squares fit of model parameters to the chordal data [6]. The analysis uses a $1\frac{1}{2}$-D transport code with diffusive and convective terms (SANCO), and a model which describes the time dependent isotope exchange between the plasma and the wall [7]. The main contribution to the 2.5 and 14 MeV neutron reactivity for these experiments was the beam-thermal reaction. The fast particle deposition profile was obtained from the self-consistent beam deposition code CHarge Exchange Analysis Package (CHEAP) [8].

The 2.5 MeV profiles predicted by both CHEAP and TRANSP are much higher in the edge than was observed in the experiment, indicating that neither code correctly calculated the fast particle profile. In each case analysed, a correction has been applied to the fast particle profile to reconcile the predicted 2.5 MeV profile with the measurement [9].

2.1. Ion transport

The $1\frac{1}{2}$-D impurity transport code Stand Alone Non-COrona (SANCO) developed at JET has been modified to treat trace amounts of tritium. SANCO solves the continuity equation, averaged over magnetic flux surfaces and using diffusive and convective (pinch) contributions to the cross-field particle transport [10]. Since discharges were in steady-state, the diffusion coefficient D and convection velocity v were time independent (ELM and sawtooth averaged) and that only the sink S_T and source Q_T were time dependent. D and v were determined in five independent zones (Fig. 2). However, because v was found to be zero within the error bars for zones 1–4, it was set to zero in all zones to minimise the scatter in the fitted values of D.

Outside the last closed flux surface (LCFS) there is a sink: $S_{T,SOL} = n_{T,SOL}/\tau_{||}$. Parallel confinement time, $t_{||}$, is taken as fixed parameter in SANCO (0.1 ± 0.05 ms) with the error propagated through the solution. This parameter determines the separatrix triton density which cannot be directly measured. In the outermost zone the pinch velocity and diffusivity are interchangeable and the absolute value is determined by the width assigned to the zone and by the tritium density assumed in the SOL model.

2.2. Tritium fraction of the neutral influx

The 14 MeV neutron signals several seconds after the puff are higher than before the puff. This can be explained

by an increase in the tritium content of the wall following the tritium gas puff. In the simulations presented here, it is assumed that immediately after the gas-puff the tritium influx from the walls steps up to a level consistent with the new steady state plasma tritium content several seconds later. From our analysis of the neutron data we know that 18–26% of the injected tritium can be found in the main plasma shortly after the tritium gas puff. The tritium which does not immediately enter the plasma will be rapidly returned to the wall, thus increasing the wall tritium concentration. A more complex dynamic wall model [7] was tested in a parameterised form in conjunction with the SANCO/CHEAP analysis but has been dropped in favour of the simpler assumption because the quality of the fit was found to be relatively insensitive to the details of the recycling model.

3. Results

Fig. 3 shows the fit between the SANCO/CHEAP model and the chordal neutron data. It is the dynamic behaviour of the triton profile such as the initial rise and decay which are dominant in deriving the diffusion coefficients. The peaking of the steady-state profile mainly determines the pinch parameters.

3.1. Transport degradation

The energy confinement time decreases by 35% with fuelling rate (Table 1) and then saturates in contrast to the deuterium fuelling efficiency ($\Delta\Gamma_{D_2}/\Delta N$) which goes almost to zero. Normalised triton content ($N_{T,plasma}/N_{T,puff}$), which could be regarded as a fuelling efficiency for tritium, shows a similar modest decrease with deuterium fuelling rate as τ_E (Fig. 4).

In L-modes, short tritium puffs produced an increment in total electron content consistent with the increase in triton content measured by the neutron detectors. A similar fraction of the injected tritium is detected inside the plasma in H-mode but in this case the electron density does not respond (Fig. 5).

The fitted triton particle diffusivity is independent of fuelling rate out to a radius of $r/a = 0.55$ (Fig. 6) and the pinch term is zero. In this region the plasma electron density profiles are slightly peaked (Fig. 7(a)) by an

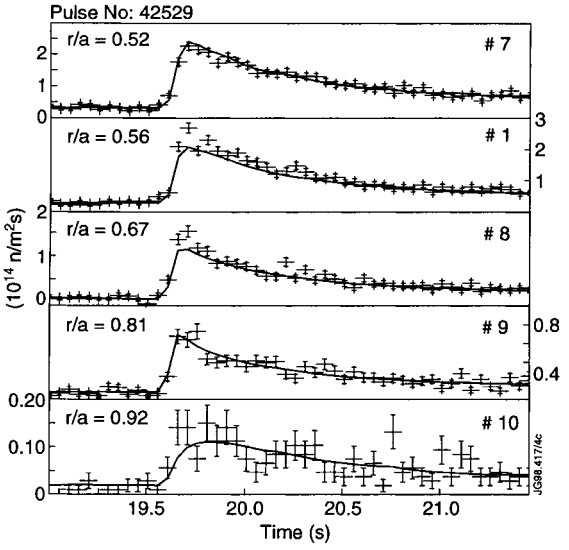

Fig. 3. Time dependence of outer neutron profile monitor channels following a short tritium gas puff. Lines of sight for these channels are shown in Fig. 2. The solid lines are the fit achieved by the SANCO/CHEAP code (overall $\chi^2 = 1.37$).

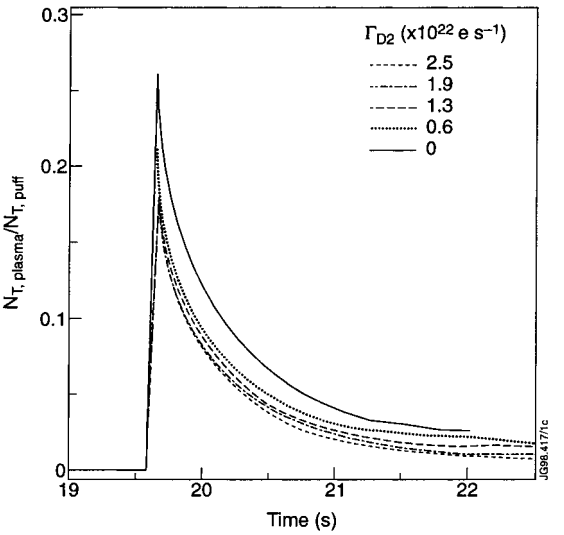

Fig. 4. Normalised triton content (background subtracted) vs. time for the deuterium fuelling scan (Fig. 1).

Table 1
Energy confinement time, plasma densities and mid-plane neutral pressure vs. external gas fuelling rate

D_2 fuelling rate, Γ_{D_2} ($\times 10^{22}$ e s^{-1})	0	0.6	1.3	1.9	2.5
Mid-plane neutral pressure ($\times 10^{-9}$ bar)	6.6	11	19	28	37
Total electron content, N ($\times 10^{21}$)	3.6	4.3	4.4	5.0	5.0
Energy confinement time, τ_E(s)	0.41	0.34	0.27	0.27	0.26
Pedestal density, n_{ped} ($\times 10^{19}$ m^{-3})	4.0	4.5	4.6	5.2	5.0
Separatrix density n_s, OSM ($\times 10^{19}$ m^{-3}), D = detached	3.2	4.5	4.5	D	D

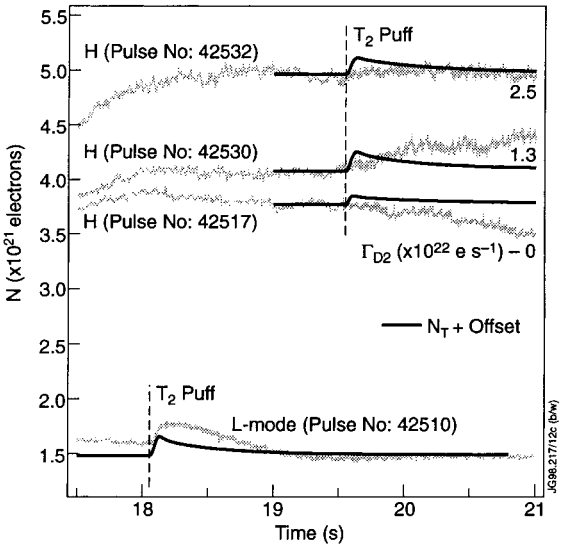

Fig. 5. Response of total electron content N in L and H-mode plasmas to trace tritium gas-puffs. Solid curves show increase which is expected from the jump in total triton content N_T as measured by the neutron diagnostics.

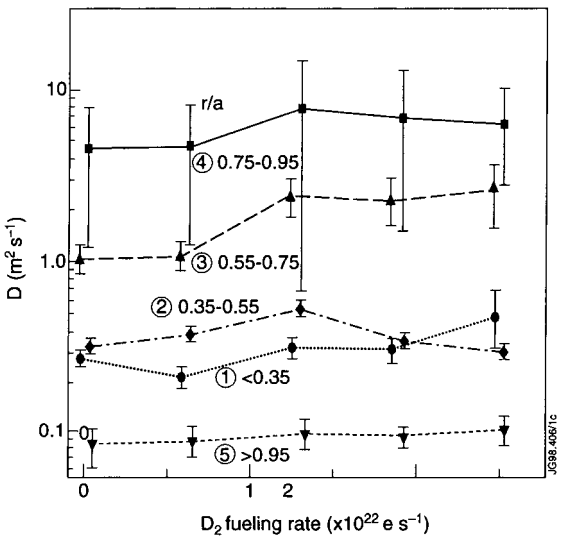

Fig. 6. Diffusivity vs. fuelling rate for the fuelling scan of Fig. 1. The radial extent of each independent transport zone is indicated in Fig. 2.

amount which seems consistent with the neutral beam particle source ($S_{NB} \sim 10^{21}$ s^{-1}). This central source is absent with RF heating and the density profiles are much flatter (Fig. 7(b)).

In a purely diffusive model, the density pedestal would be a consequence of a balance between ionisation sources inside the separatrix at the ionisation depth Δ_{iz}

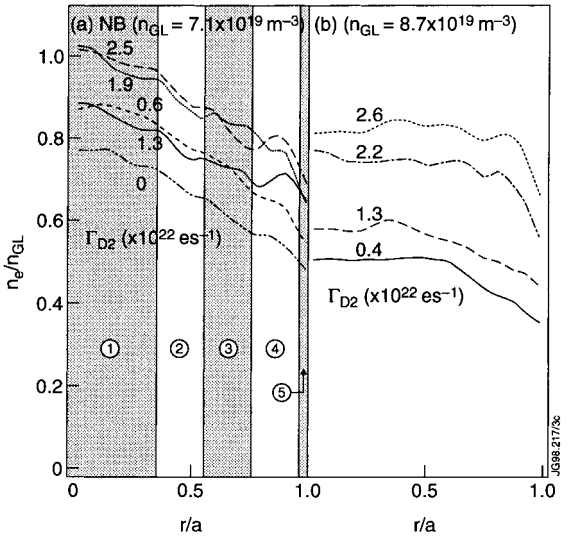

Fig. 7. (a) Density profiles for the fuelling scan of Fig. 1 and (b) the much flatter density profiles obtained in a fuelling scan with RF heating.

and radial diffusion out to the SOL. EDGE2D/NIMBUS [11] simulation of pulse 42529 (see Fig. 1) shows that the ionisation source inside the separatrix is $\sim 3 \times 10^{21}$ m^{-3} s^{-1} which is three times the neutral beam fuelling rate but with an initial decay length of 1 cm. A balance between the ionisation source inside the separatrix, S_{iz}, and cross field diffusion, D, increases the density from the separatrix, n_s, to the pedestal, n_{ped}, by: $n_{ped} - n_s = S_{iz}\Delta_{iz}/(AD)$, where A is the plasma surface area.

Both the divertor and main chamber neutral pressure and D_α a intensity increase with deuterium fuelling rate by a factor 5–10 (Table 1). Assuming a corresponding increase in the main plasma ionisation source S_{iz} then the observed density rise of 25% would require at least a factor 4 increase in edge diffusivity.

The transport analysis indicates that when the deuterium fuelling rate is increased there is no change in particle diffusivity (or alternatively the inward pinch) in the pedestal region which contributes ~65% to the central density and no change in the penetration probability for tritons. Two assumptions affect the validity of the transport results for the pedestal: (1) the separatrix triton density is assumed small compared to the main plasma and that this situation does not change with fuelling rate (see Section 3.2) and (2) that the width of the tritium density pedestal does not depend on fuelling rate.

In the outer half of the plasma ($0.95 > r/a > 0.55$) which contributes ~20% to the central density the diffusivity roughly doubles with a dependence on fuelling rate similar to that of τ_E. In the inner half of the plasma ($r/a < 0.55$) which contributes ~15% to the central

density (in NBI heated discharges) there is no change in the transport.

3.2. Ion fuelling and SOL behaviour

Analysis of the separatrix electron density, $n_{s,OSM}$, for the fuelling scan of Fig. 1 has been carried out using the "Onion-Skin" method (OSM) [12] (Table 1). One-dimensional solutions are computed for each flux tube with the divertor Langmuir probe data used as the boundary condition [13]. It is applicable to inter-ELM periods where the plasma is attached.

The separatrix electron density increases for the first fuelling step and then saturates at a value close to that of the pedestal [12]. At a fuelling rate of 1.9×10^{22} e s^{-1} the plasma detaches strongly between ELMs and the OSM is no longer applicable.

The OSM results suggest that in the trace tritium experiments the separatrix density was close to the pedestal density and hence the major contributor to the total plasma electron content. If the separatrix triton density behaves in a similar way then it invalidates the assumption of low separatrix density used in the trace tritum analysis and implies a degradation of pedestal diffusivity with deuterium fuelling rate, or diminishing penetration depth for neutrals.

4. Discussion and conclusions

In contrast to L-mode plasmas it is clear that the H-mode electron density is strongly clamped. The trace tritium results show that this is not due to a failure of the ions produced by gas-fuelling to penetrate the main plasma. At the same time the transport analysis shows that while there is some particle transport degradation in the outer half of the plasma, proportional to the degradation in global energy confinement time, it cannot explain the density saturation. This is not only because the changes do not appear to be large enough or have the right dependence with fuelling rate but also because the most significant contribution to the total electron content comes from the pedestal region. The lack of a diagnostic for tritium at trace concentrations in the SOL means that the transport analysis cannot tell us anything definitive about transport in the pedestal. However, we have used the OSM to study the relationship between the separatrix and pedestal electron densities. This shows that the density pedestal rapidly disappears as the deuterium fuelling rate rises until the dominant contribution to the main plasma density comes from the separatrix. Hence degradation of edge particle transport or reduced ionisation depth play a role but the ultimate clamping of the total electron content seems to result from saturation of the separatrix density. Detachment between ELMs is observed in this condition and lends general support to idea that the ultimate cause of density saturation lies in SOL physics [4]. However, the results do not confirm or deny any specific model for this process.

The trace tritium transport analysis represents an average over ELMs and sawteeth. It seems likely that ELMs are somehow involved in the process of density saturation. In some *but not all* cases the tritium puff provokes transient changes in ELM behaviour.

In contrast to the edge region, the inner half of the plasma appears to be dominated by diffusive transport with the density peaking being a result of central fuelling with neutral beam particle sources. Central fuelling thus appears to be an effective way to raise the central density in H-mode.

The H-mode density limit and the low fuelling efficiency which it implies is a concern for edge fuelled tritium in ITER. However, JET trace tritium results show that tritons produced by gas fuelling penetrate with high efficiency. In addition, the tritium reaches the core in a time comparable with energy confinement time. Hence active DT mixture control should be possible by gas fuelling in ELMy H-modes even though the total plasma electron content is clamped by processes which are still not understood.

References

[1] M. Greenwald et al., Nucl. Fusion 28 (1988) 2199.
[2] S. Putvinski, R. Aymar, D. Boucher, C.Z. Cheng et al., in: Proceedings of the 16th International Conference on Fusion Energy Montreal IAEA-CN-64/F-1, Vol. II, 1996, p. 737.
[3] G. Saibene, B. Balet, S. Clement et al., Europhysics Conference Abstracts, Vol. 21A Part I, 1997, p. 49.
[4] K. Borrass, J. Lingertat, R. Schneider, Contrib. Plasma Phys. 38 (1998) 130.
[5] O.N. Jarvis, J.M. Adams, F.B. Marcus, G.J. Sadler, Fusion Eng. Des. 34&35 (1997) 59.
[6] K.-D. Zastrow et al., Particle transport in steady-state ELMy H-modes studied by trace tritium injection during JET DTE-1, in: 25th EPS Conference on Controlled Fusion and Plasma Physics, Prague, 1998.
[7] J. Ehrenberg, Physical Processes of the Interaction of Fusion Plasma with Solids, Academic Press, New York, 1996, p. 35.
[8] M.G. von Hellermann et al. in: P.E. Stott, G. Gorini, E. Sindoni (Eds.), Diagnostics for Experimental Thermonuclear Fusion Reactors, Plenum, New York, 1996, p. 281.
[9] K.-D. Zastrow, P. Andrew, N.P. Basse, P. Breger et al., in: 25th EPS Conference on Controlled Fusion and Plasma Physics, Prague, 1998.
[10] K. Lackner, K. Behringer, W. Engelhardt, R. Wunderlich, Naturforsch. 37A (1982) 931.
[11] A. Taroni et al., J. Nucl. Mater. 220–222 (1995) 1086.
[12] S.J. Davies et al., these Proceedings.
[13] P.C. Stangeby et al., J. Nucl. Mater. 241–243 (1997) 358.